

Preparation and Morphology Study of Electrospun Cellulose Acetate Fibers Using Various Solvent Systems and Concentrations

Wasan Alkaron^{1,2,3}, Alaa Almansoori^{1,3}, Katalin Balázsi¹, Csaba Balázsi^{1*}

¹ Institute for Technical Physics and Materials Science, HUN-REN Centre for Energy Research, Konkoly-Thege Miklós str. 29–33, H-1121 Budapest, Hungary

² Doctoral School of Materials Science and Technologies, Óbuda University, Bécsi str. 96/B, H-1034 Budapest, Hungary

³ Technical Institute of Basra, Southern Technical University, Zubair Road, 61001 Basra, Iraq

* Corresponding author, e-mail: balazsi.csaba@ek.hun-ren.hu

Received: 04 June 2025, Accepted: 05 August 2025, Published online: 11 September 2025

Abstract

This research investigates the application of electrospinning in the production of CA fibers and examines how two critical parameters influence the morphology and dimensions of the resulting CA products during the spinning process. These factors include the solvent system employed and the concentration of the solution. By analyzing these parameters, the research aims to elucidate their effects on the characteristics of the resultant CA materials following the spinning process. The study employed acetone as a single-solvent system, while acetone–acetic acid (2:1) and acetone–chloroform, N,N-dimethylformamide (DMF) (2:1) were used as mixed-solvent systems at room temperature. For the single-solvent approach, CA was dissolved in acetone at concentrations of (5, 10, 11, 13, and 15 wt%). In the co-solvent systems, CA was dissolved in acetone–DMF (2:1) at concentrations of (5, 10, 15, 16, 18, and 20 wt%), and in acetone–acetic acid (2:1) at concentrations of (5, 10, 15, and 20 wt%). Although DMF and acetic acid could dissolve CA to form clear solutions (at 5 wt%), electrospinning primarily resulted in discrete beads. In contrast, electrospinning CA in acetone produced short, beaded fibers. The optimal results, yielding continuous fibers without beading, were achieved with 10 wt% CA in acetone, 15 wt% CA in acetone/acetic acid (2:1), and 18 wt% CA in acetone/DMF (2:1). The results revealed how various parameters affected the diameter and quality of the fibers, ultimately determining the optimal conditions.

Keywords

electrospinning, cellulose acetate, polymer concentration, fiber morphology

1 Introduction

Electrospinning is an intriguing method for creating fibers with diameters that can range from micrometers to nanometers [1–3]. These fibers are utilized in a variety of fields, such as tissue engineering [4–6], filtration [7], wound dressings [8], and drug delivery systems [9]. In recent years, there has been a significant increase in interest in cellulose acetate (CA) nanofibrous materials as a product derived from natural and renewable resources, particularly with the advent of electrospinning [10]. CA-based materials are biodegradable, renewable, and considered safe for humans and the environment [11].

During electrospinning, parameters can be adjusted to manipulate fiber diameters, surface characteristics, shapes, and alignments. The size and morphology of fibers are affected by the polymer's composition and the electrospinning

parameters [12]. Polymer concentration in the solution is an important factor in determining fiber diameter, as fiber diameter relates to viscosity in the solution [13–15]. Additionally, the choice of solvent and mixed solvent affects the fiber size and continuous electrospinning of CA fibers. The use of CA solution in acetone and water under acidic conditions results in larger fibers, while in the case of basic conditions, finer fibers are produced [16–18]. Besides the various binary mixtures, a ternary mixture of acetone–dimethylformamide (DMF)–trifluoroethylene (TFE) can also be employed to prepare a CA solution. Electrospun fibers from this mixture range in diameter from approximately 200 nm to about 1 μm [19].

The substitution of hydroxyl (OH) groups on the cellulose chain with acetyl groups make CA being less

hydrophilic than cellulose. Electrospun CA mats can vary in hydrophobicity depending on the fiber diameter and chemical changes during electrospinning [20]. Fiber diameter appears to have an inverse relationship with hydrophilicity in CA nanofibers. As the fiber diameter decreases to the nanometer range, the hydrophilicity of the CA nanofibers tends to increase. This is evidenced by the water contact angle measurements reported by Selatle et al. [21]. The present study provides extensive insight into the effects of various solvents, concentrations, and processing parameters on the appearance and/or size of CA products as spun. The morphology as well as wettability and swelling properties of the CA fiber are studied to understand how processing conditions affect their performance. In this study, acetone was used as a single solvent, whereas acetone/acetic acid and acetone/DMF were mixed solvents. In addition, we choose the best conditions based on their unique asymmetric characteristics in terms of continuous fiber production, fiber size, and wettability.

2 Materials and methods

CA, a white powder with a molecular mass of 29,000 Da, acetyl content of 40% (w/w), and degree of acetyl substitution of approximately 2.4 purchased from Sigma-Aldrich (USA). CA with low molecular mass of 29,000 was selected due to factors such as its solubility and prior optimization studies. In contrast, lower-molecular-mass polymers generally require higher concentrations for electrospinning to maintain sufficient chain entanglement.

The study utilized solvents including acetone purchased from Fisher chemical (Finland), acetic acid sourced from VWR chemical (Finland), and N,N-DMF, sourced from Molar chemicals Kft. All the chemicals were employed in the experiments as-received state without additional purification processes.

3 Preparation of homogeneous viscous CA solution

Spinning solutions were prepared at ambient temperature using either a single solvent or a combination of solvents. In the single solvent method, CA powder was dissolved in acetone at varying concentrations (5, 10, 11, 13, and 15 wt%) by stirring until a uniform solution was formed. To explore the effects of mixed solvent systems, two combinations were tested: acetone/acetic acid (2:1) with CA concentrations of (5, 10, 11, 13, and 20 wt%) and acetone/DMF (2:1) with CA concentrations of (5, 10, 15, 16, 18, and 20 wt%). The process involved adding CA to the selected solvent system and mixing it with continuous

stirring at 800 rpm until a clear, homogeneous viscous solution was achieved. The concentrations of CA polymers dissolved in different solvents are detailed in Table 1.

CA concentrations of 5%, 10%, 15%, and 20% (w/v) were initially involved in each solvent system to prepare the polymer solution. The concentration ranges were further adjusted by exploring intermediate concentrations, such as 11% and 13%, and high concentrations of 16% and 18%. This approach, therefore, enables the use of different sets of polymer concentrations for different systems to ensure electrospinnability and fiber quality. All CA solutions were electrospun immediately after preparation to avoid polymer chain relaxation or solvent–polymer interactions.

4 Electrospinning of CA fibers

During electrospinning, a viscous polymeric solution is subjected to high voltage, which accumulates charges and causes the solution to stretch, resulting in a jet of charged fibrous structures caused by repulsive forces. Simultaneously, an electrostatic field is formed between the needle and the collector, the schematic diagram of the electrospinning shown in Fig. 1 [10].

Electrospinning was performed using 10 mL plastic syringes fitted with 22-gauge blunt-tip needles (Hamilton Company, Reno, NV, USA), which served as spinnerets. The setup comprised a high-voltage power supply (ES30P-6W, Gamma High Voltage Research, Inc., Ormond Beach, FL, USA) operating between 7 and 20 kV, a syringe pump (KD

Table 1 Solution parameters of spun fibers

Concentration of CA%	Acetone	Acetone/acetic acid	Acetone/DMF
5, 10, 11, 13, 15, 20	100%	–	–
5, 10, 15, 20	–	70/30	–
5, 10, 15, 16, 18, 20	–	–	70/30

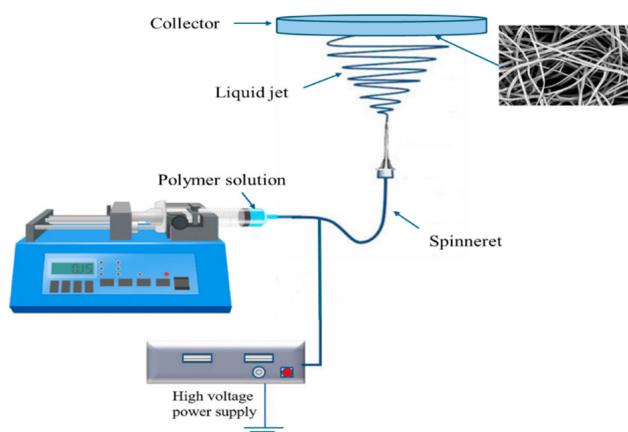


Fig. 1 Schematic diagram of the electrospinning process [10]

Scientific, Model 200) dispensing at rates of 30–100 $\mu\text{L}/\text{min}$, and a grounded aluminum foil collector. All experiments were conducted at constant ambient temperature. To mitigate the rapid evaporation of acetone and prevent needle-tip clogging caused by polymer accumulation, airflow around the spinneret was eliminated. This precaution helped maintain jet stability and ensured continuous fiber formation. To ensure consistent fiber formation, the needle tip was meticulously cleaned between each electrospinning run, even in the absence of airflow. The electrospinning parameters, including the spinning distance, operating voltage, and flow velocity, were adjusted for each solvent system, as shown in Table 2. Following fabrication, the resulting nanofibrous mat was collected on aluminum foil and stored for subsequent characterization.

The difference in flow rate solvent systems during electrospinning is primarily due to differences in the physico-chemical properties of the solvent mixtures, which affect the electrospinnability of the polymer solution. Each flow rate range is optimized to match the stability of the electrospinning jet for each solvent system.

5 Characterization

5.1 Scanning electron microscope (SEM) and fiber diameter

The morphology of the as-spun materials was investigated at high resolution using scanning electron microscopy (SEM) with a Scios2 Dual-Beam SEM (manufacturer: Thermo Fisher Scientific, USA) equipped with an X-MAX-20 EDS detector (Oxford Instruments, Abing, UK). SEM specimens were prepared by cutting Al sheets layered with as spun fibers and carefully fixing the cut sections to copper stubs. In addition, Java-based image processing software (ImageJ) [22] was used to determine the average fiber diameter across a range of electrospinning conditions.

5.2 Water contact angle measurement

The concept of wettability is conceptualized through the behavior of a liquid drop on a surface, where it assumes

Table 2 Electrospinning parameters used in experiments

Solvent system	Acetone	Acetone/acetic acid	Acetone/DMF
	Spinning distance 10 cm	Spinning distance 10 cm	Spinning distance 12 cm
Electrospinning parameters	Operating voltage 18–20 kV	Operating voltage 19–20 kV	Operating voltage 20 kV
	Flow velocity 0.5–1 mL/h	Flow velocity 1–1.5 mL/h	Flow velocity 0.4–0.8 mL/h

a distinct shape at an angle θ relative to the surface. The interaction between the liquid and the solid is quantified by the cosine of the equilibrium contact angle (θ) for a particular liquid. This equilibrium contact angle functioned as an indicator to assess the wettability characteristics of the surface.

The wettability of the electrospun meshes was assessed by contact angle measurements using an adjustable-volume pipette, and sample equipment was employed for the procedure. Distilled water was used as a liquid medium. Approximately 2 mL of distilled water was dispensed per drop. The droplet took 5 s to stabilize on the surface before its image was captured. Analysis of the images and measurement of contact angles were performed using ImageJ software [22]. The software computed the contact angle by assessing the tangent of the droplet's outline without limiting its volume. The edges of the droplet and the tangent were each measured three times. ImageJ's manual [22] detection method involved placing specific points along the droplet's edge to define its outline. After selecting these points, the software automatically identified the best-fit profile. Fig. 2 presents a schematic diagram illustrating how the θ was analyzed using the ImageJ [22].

5.3 Swelling in water

To evaluate their potential as carriers for topical and/or transdermal drug delivery, electrospun CA fiber mats were subjected to additional analysis. This involved measuring their swelling in distilled water. The process began by cutting the newly spun fiber mats into $2 \times 2 \text{ cm}^2$. These samples were then immersed in 50 mL of distilled water within sealed containers and kept at room temperature. To assess swelling, the specimens were weighed after 24 h of immersion in water. Subsequently, they were dried in a vacuum

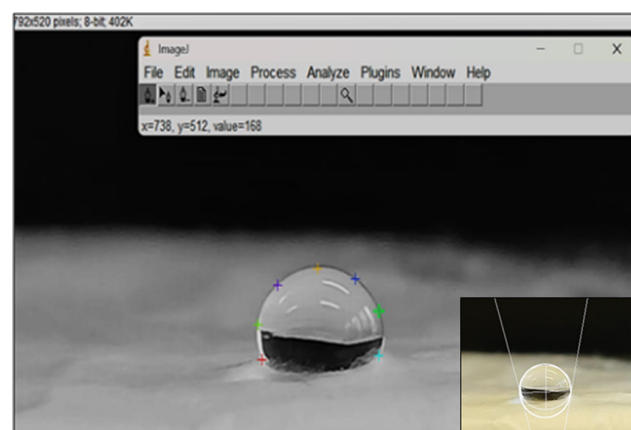


Fig. 2 Contact angle measurement analyzed by ImageJ software [22]

oven at 50 °C for 1 h and weighed again to determine their dry mass. The swelling percentage was calculated in Eq. (1):

$$\text{Swelling (\%)} = \frac{(W - W_d)}{W_d} \times 100, \quad (1)$$

where W represents the mass of each sample after being submerged in water, while W_d denotes the dry mass of the sample following the drying process in the oven.

6 Results and discussion

6.1 SEM and fiber diameter for acetone solutions

Acetone was selected as the solvent for dissolving CA powder due to its high volatility and compatibility with CA [23]. Solutions were prepared at concentrations ranging from 5 to 15 wt%, and a moderate flow rate (0.5–1 mL/h) was employed to balance evaporation and jet stability. Their electrospinnability was then evaluated. As shown in Fig. 3, the 5 wt% CA solution formed a clear, homogeneous mixture, yet electrospinning yielded only particulate deposits on the collector, with SEM imaging confirming beaded morphologies rather than continuous fibers. This aligns with previous studies reporting that excessively low polymer concentrations (<8 wt%) in volatile solvents often result in bead formation due to insufficient chain entanglement for stable jet elongation [24]. The inability of 5 wt% CA spinning dopes to form continuous fibers Fig. 3, (5 % CA low/high magnification) is consistent with prior studies by Jaeger et al. [25], and Liu

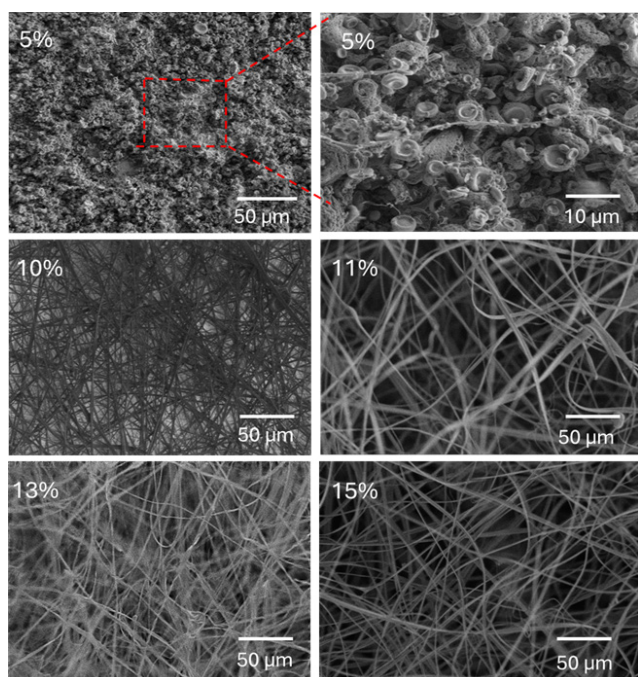


Fig. 3 Effect of CA concentration in acetone on the morphology of electrospun CA fibers

and Hsieh [26] who observed that low-concentration CA solutions (≤ 5 wt%) in acetone predominantly yield beaded or fragmented morphologies rather than uniform fibers. This phenomenon arises from insufficient chain entanglement at low polymer concentrations, which is critical for stabilizing the electrospinning jet against capillary breakup [27]. Below the critical entanglement concentration, polymer chains lack adequate intermolecular interactions to sustain fiber elongation, resulting in Rayleigh instability-driven bead formation [28].

When the CA concentration was increased to 10 wt%, fine, continuous fibers with an average diameter of 0.875 μm were successfully produced. Further increasing the concentration to 11 wt% eliminated bead formation entirely, yielding smoother fibers with a larger mean diameter of 1.747 μm , indicating improved polymer chain entanglement. At even higher concentrations (13 wt% and 15 wt%), the average fiber diameters increased to 2.271 μm and 3.172 μm , respectively, as evidenced in Figs. 3 and 4. This trend confirms that higher polymer concentrations promote the transition from beaded fibers to

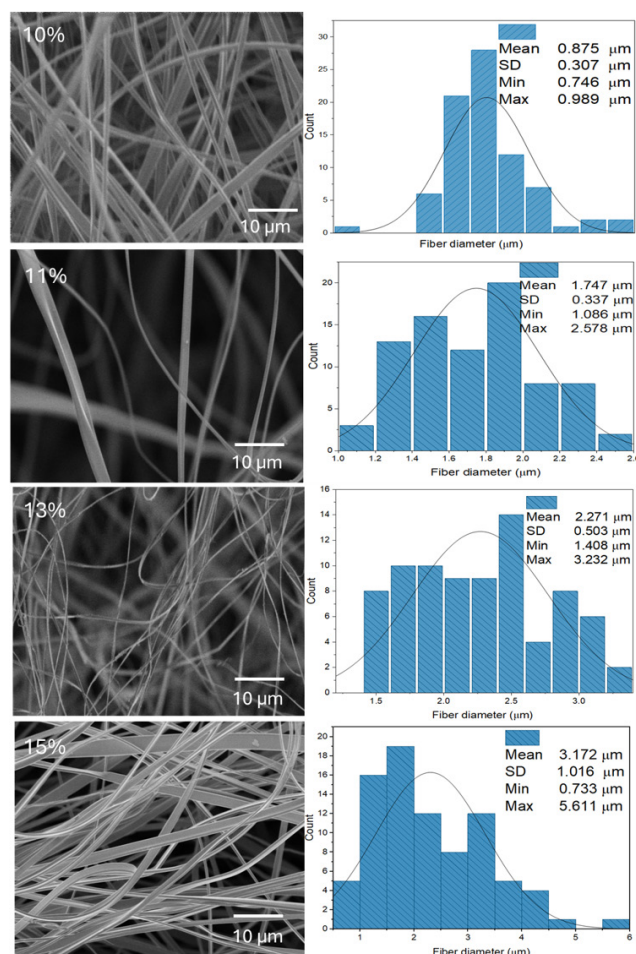


Fig. 4 SEM images and their corresponding diameter distribution of fibers electrospun from acetone solvent system

uniform, continuous fibers due to enhanced chain entanglement and reduced instability during jet formation [29]. Based on these observations, CA concentrations between 10–15 wt% are optimal for producing defect-free fibers. Notably, 10 wt% CA in acetone produced the continuous fibers without beads, suggesting an ideal balance between polymer solubility and solvent evaporation rate.

However, when the concentration was raised to 20 wt%, electrospinning became unfeasible due to rapid needle tip clogging. This failure is attributed primarily to the excessive viscosity of the solution, compounded by the high evaporation rate of acetone, which led to premature polymer solidification at the spinneret. While surface tension may play a role, the dominant factor appears to be the formation of a highly viscous semi-solid at the needle tip, preventing stable jet formation. These findings highlight the critical role of solution viscosity and solvent volatility in electrospinning, emphasizing that optimal CA concentrations must balance spinnability and fiber morphology [30].

The electrospinning of CA solutions in acetone can be enhanced by introducing a co-solvent or modifying the liquid, primarily to address clogging issues. Research by Sayed et al. [31] demonstrated that adding DMF resulted in the formation of fibers with beads.

Interestingly, additional acetic acid to acetone improved the process. A study using a 3:1 acetic acid/water mixture for CA electrospinning enhanced the electrospinnability of CA solutions in acetone/acetic acid mixtures. This suggests that acetic acid plays a role in fiber formation, even if it requires combination with other solvents for optimal results [32]. CA fiber mats produced through electrospinning can serve as delivery systems for topical applications as it can facilitate the transdermal release through the skin making them more appropriate for wounds and skin care applications. A range of solvent combinations is available for this process. The production of CA fibers *via* electrospinning is an ongoing process. More investigation is needed to fully comprehend the potential of this methodology [33, 34].

6.2 SEM and fiber diameter for mixed solutions

6.2.1 Acetone and acetic acid

To reduce the fast evaporation of acetone, acetic acid was added in various proportions. CA solutions at a concentration of 5, 10, 15, 20 wt% were prepared in 2:1 (v/v) acetone/acetic acid. The presence of acetic acid increases the solution viscosity, which contributes to a more stable electrospinning process and supports the use of a higher flow rate in the range of 1–1.5 mL/h. It was observed that dope solutions with 5 wt% CA produced fibers with significant bead formation

as shown in Fig. 5, which can be attributed to insufficient molecular entanglement and low solution viscosity [31, 35].

At a concentration of 10 wt%, short, fine fibers with noticeable beading were formed, consistent with previous studies on low-concentration polymer solutions in electrospinning. However, the 20 wt% CA solution led to a non-continuous jet due to excessive viscosity, frequent spinneret clogging, and reduced fiber mat production efficiency [36, 37]. In contrast, the 15 wt% CA solution exhibited optimal spinnability, producing a continuous jet and smooth, bead-free fibers, as demonstrated in Fig. 5. This aligns with findings by Angel et al. [36], who reported that increasing polymer concentration enhances spinnability and reduces fiber beading by improving chain entanglement and solution stability.

SEM analysis in Fig. 6 revealed that fiber diameters increased systematically with solution concentration [38–40]. Specifically, the average diameter increased from 0.7 μm (10 wt%) to 3.8 μm (20 wt%), as summarized in Table 3. This trend is consistent with electrospinning studies showing that higher polymer concentrations increase solution viscosity, hindering fiber stretching and resulting in thicker fibers with broader diameter distributions [41].

Additionally, the increase in fiber diameter at higher CA concentrations may be linked to enhanced solution conductivity. Higher conductivity increases the electrostatic force acting on the jet, accelerating its travel toward

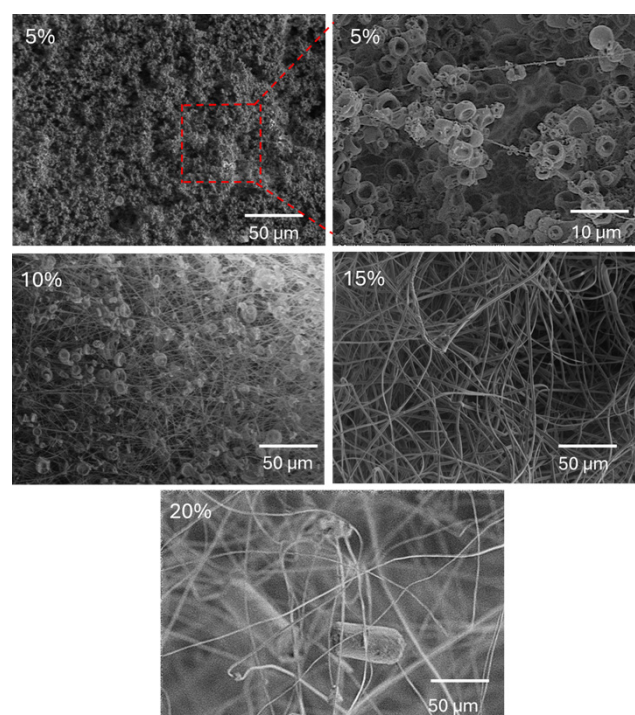


Fig. 5 Effect of CA concentration in acetone/acetic acid (2:1) on the structure of the electrospun CA fibers

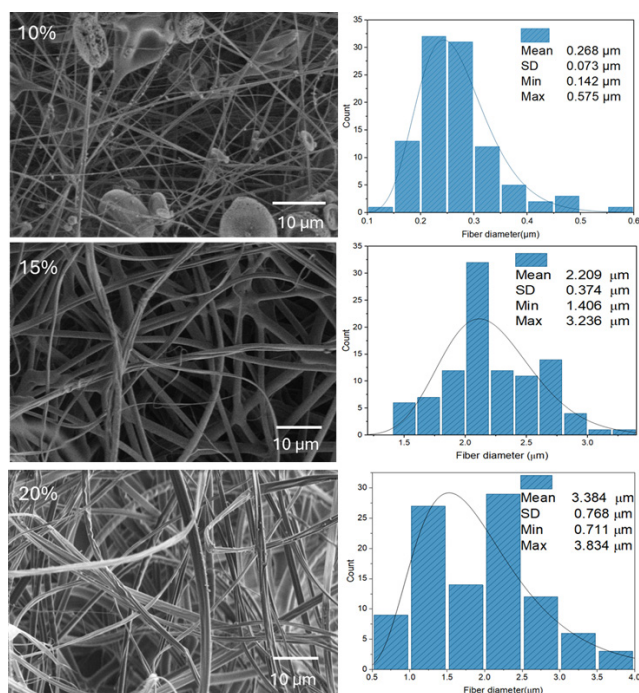


Fig. 6 SEM images and their corresponding diameter distribution of fiber electrospun from acetone/acetic acid solvent system

Table 3 Evaluation of fiber produced from different solvents and different concentration

Solvent system	Concentration of CA (%)	Mean fiber diameter (μm)	Fiber evaluation
Acetone	5	–	Bead
	10	0.875	Good fiber
	11	1.747	Fiber
	13	2.271	Fiber and bead
	15	3.172	Fiber and a lot of beads
Acetone/acetic acid	20	–	No fiber
	5	–	Bead
	10	0.268	Fiber and bead
Acetone/DMF	15	2.209	Good fiber
	20	3.834	Fiber and bead
	5	–	Beads
	10	–	Beads
	15	–	Short fiber and beads
	16	0.321	Fiber and beads
	18	0.522	Fiber
20	0.793	Fiber and beads	

the collector [24, 42]. As a result, bending instability occurs closer to the collector, shortening the jet's path trajectory and reducing Coulombic and bending stresses. However, these parameters were not measured experimentally, as this study focused primarily on the morphological

outcomes of the produced fibers rather than on a detailed analysis of the solvents.

Moreover, increased electrostatic forces can enhance mass throughput, further contributing to thicker fiber formation. The combination of acetone and acetic acid provides a versatile solvent system for producing CA nanofibers with controllable morphology and dimensions [43]. Previous studies have demonstrated that acetic acid not only moderates solvent evaporation but also influences solution conductivity and polymer chain interactions, enabling fine-tuning of fiber properties. Thus, optimizing the solvent composition and polymer concentration is crucial for achieving desired electrospun fiber characteristics [44, 45].

6.2.2 Acetone and DMF

To investigate the effect of polymer concentration and solvent composition on the morphology of CA fibers, solutions with concentrations of 5, 10, 15, 16, 18, and 20 wt% were prepared using a 2:1 acetone/DMF solvent system. A flow rate of 0.4–0.8 mL/h was employed, as the higher viscosity of the acetone/DMF mixture necessitates a lower rate to ensure a stable and continuous jet during electrospinning.

At lower concentrations (5 and 10 wt%), the electrospinning process resulted in the formation of thin films on the collector, accompanied by bead formation. In contrast, a 15 wt% polymer solution produced dense, large beads interspersed with fine fibers, as illustrated in Fig. 7 (low

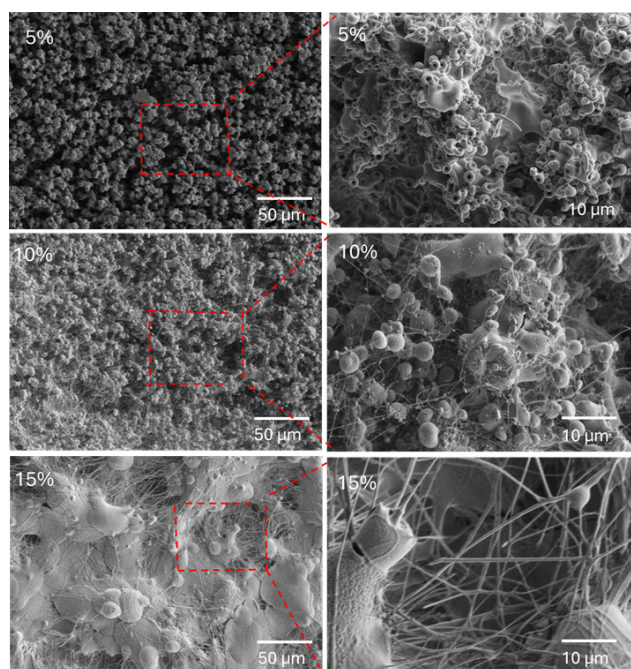


Fig. 7 Effect of CA concentration in acetone/DMF (2:1) on the structure of the electrospun CA fibers at different magnification

and high magnification). The formation of beaded fibers was more pronounced at lower CA concentrations, likely due to insufficient polymer chain entanglements, which destabilized the electrospinning jet. However, as the concentration increased to a critical threshold, the bead density decreased, suggesting improved solution stability and fiber uniformity [16, 37, 46, 47].

For instance, short fibers with an average diameter of 0.32 μm were observed in samples produced from 16 wt% CA solutions Table 2. Increasing the polymer concentration to 18 wt% led to more consistent fiber formation, along with a relatively uniform size distribution, yielding fibers averaging 0.52 μm in diameter Figs. 8 and 9.

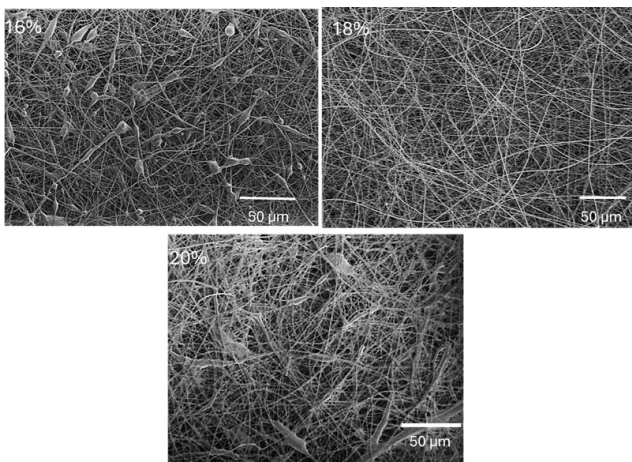


Fig. 8 Effect of CA concentration in acetone/DMF (2:1) on the structure of the electrospun CA fibers

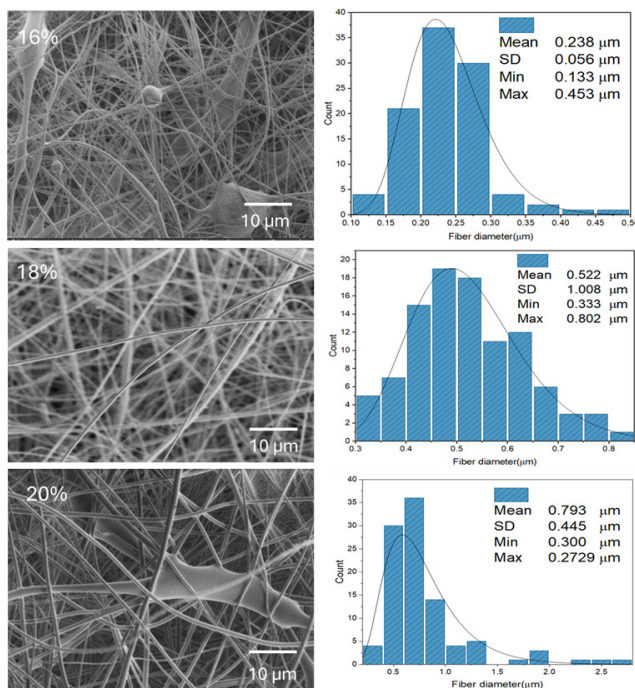


Fig. 9 SEM images and their corresponding diameter distribution of fibers electrospun from acetone/DMF solvent system

This improvement can be attributed to enhanced polymer chain entanglements, either in concentrated or semi-diluted solutions which play a crucial role in stabilizing the electrospinning jet and defining fiber morphology [48, 49].

However, when the CA concentration increased to 20 wt%, bead formation occurred alongside fiber production due to the high viscosity of the solution. Despite this, controlled fiber generation (mean diameter: 0.79 μm) was still achievable using a syringe pump to regulate the feeding rate in the 2:1 acetone/DMF solvent system. At elevated concentrations, the high viscosity of the CA solution impedes flow without external force application [19]. Based on these observations, the critical CA concentration for producing continuous, bead-free fibers with a homogeneous size distribution was determined to be approximately 18 wt% in the 2:1 acetone/DMF system.

6.3 Contact angle

The measurement of contact angles serves as a powerful diagnostic tool for characterizing wetting behavior and interfacial heterogeneities in fibrous materials. For electrospun CA membranes, precise control over surface hydrophilicity-hydrophobicity is crucial for tailoring performance in applications ranging from water filtration to biomedical scaffolds [50]. Fig. 10 (a) to (c) systematically presents how solvent selection and polymer concentration govern the wetting properties of CA fibers through contact angle analysis. In acetone-based systems Fig. 10 (a), the initial contact angle of 81° confirms hydrophilic. The observed decrease to 61.5° at 15 wt% polymer concentration aligns with the established relationship between fiber diameter and wettability. Lower concentrations produce finer fibers with higher surface roughness, enhancing apparent hydrophobicity [51]. Conversely, higher concentrations yield larger diameters with smoother surfaces that promote water spreading, as demonstrated by Koombhongse et al. [52]. The acetone/acetic acid (2:1) system Fig. 10 (b) exhibited similar hydrophilic trends (77° \rightarrow 65.3°), where acetic acid's additional hydrogen bonding capacity further enhanced surface hydration [53].

Most remarkably, acetone/DMF (2:1) formulations Fig. 10 (c) displayed concentration-dependent wettability switching (102° \rightarrow 85.6°). The initial hydrophobicity ($\theta > 90^\circ$) stems from DMF's aprotic nature promoting acetyl group surface orientation [54]. However, as concentration increases to 20 wt%, chain entanglement forces hydrophilic backbone segments toward the interface – a molecular rearrangement phenomenon extensively characterized by Thielke et al. [55].

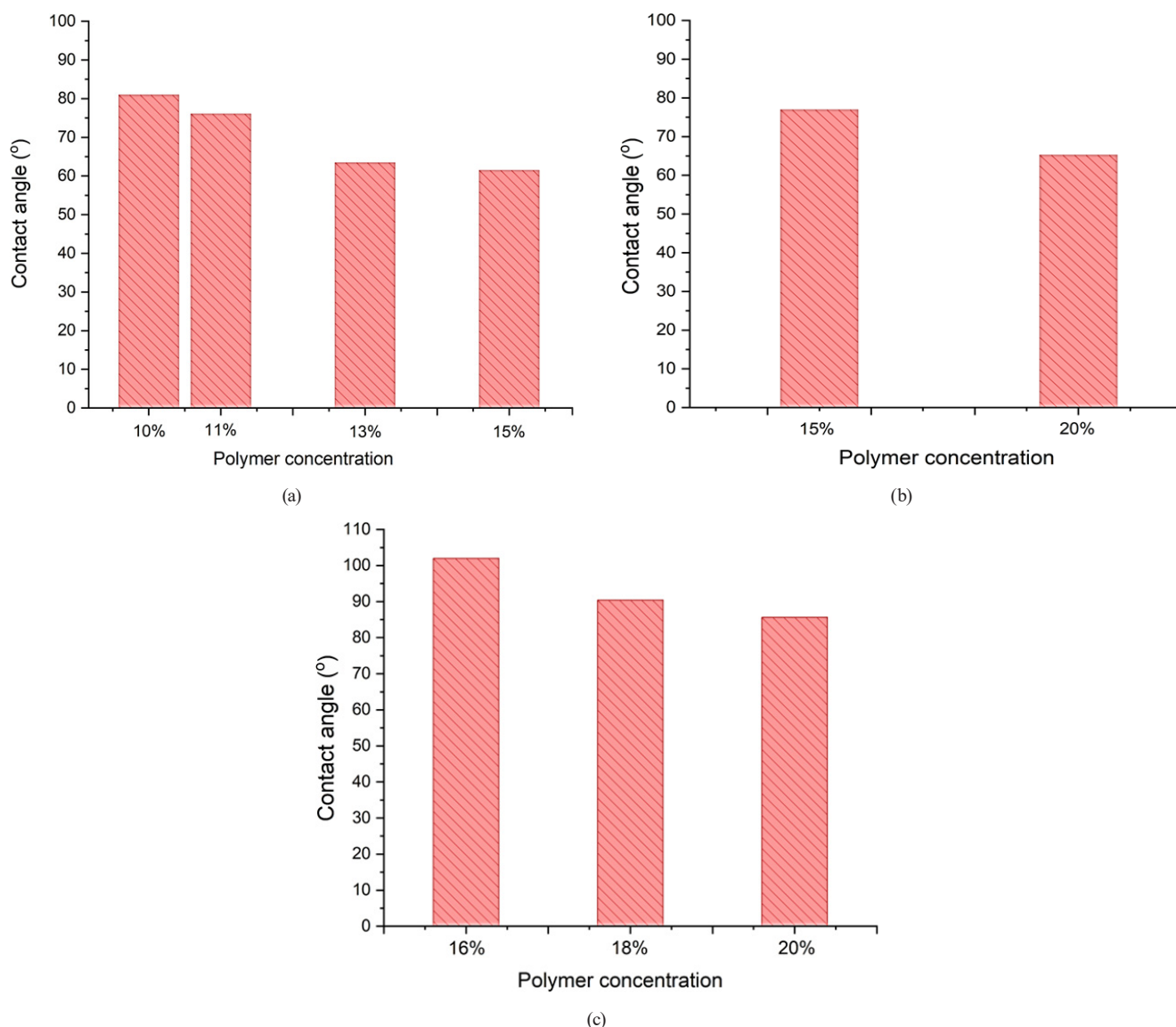


Fig. 10 Contact angle as a function of polymer concentration used for preparation of spinning solutions of CA from different solvent mixture: (a) acetone; (b) acetone/acetic acid (2:1); (c) acetone/DMF ratio (2:1)

To further evaluate the wetting behavior of the electrospun CA fibers, time-resolved contact angle measurements were performed over a 15-min period on selected samples: 10 wt% CA in acetone, 15 wt% CA in acetone/acetic acid (2:1), and 18 wt% CA in acetone/DMF (2:1). A sequence of images was recorded to monitor droplet spreading over time. As shown in Fig. 11, a progressive reduction in contact angle was observed across all samples, indicating dynamic wetting behavior. The choice of solvent system significantly influenced the initial and time-dependent contact angle values, consistent with findings reported in earlier studies [56]. Among the tested samples, the CA fibers electrospun from 15 wt% CA in acetone/acetic acid exhibited the smallest water contact angles, suggesting enhanced hydrophilicity. This can be

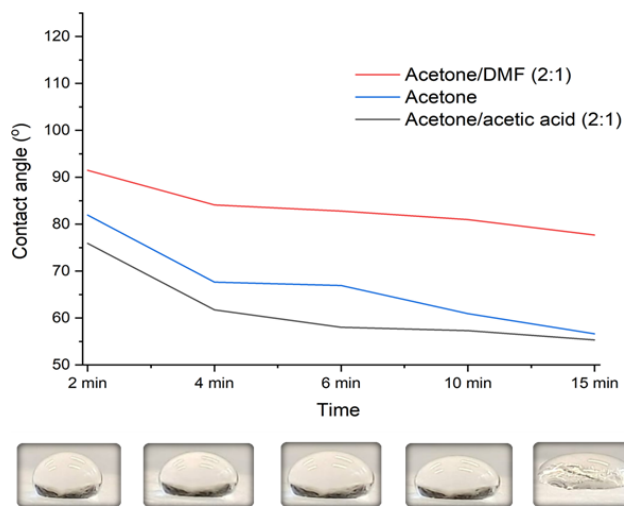


Fig. 11 Variation of contact angle as a function of time for selected fibers in different solvent systems

attributed to a combination of smaller average fiber diameter and greater porosity, which facilitates capillary-driven water absorption. As observed in similar cellulose-based systems, the swelling of the fiber matrix also plays a role in accelerating liquid penetration [57]. Moreover, while fiber diameter directly affects wetting by controlling capillary dimensions, it also indirectly influences contact angle through its effect on surface roughness [58].

The reduction in contact angle over time was attributed to water infiltration into the fibrous mat, aided by pore connectivity and swelling of the CA fibers. As water filled the inter-fiber pores, the surface tension between the droplet and the fiber network decreased, enhancing spreading [59]. The results suggest that CA fibers exhibit favorable wetting characteristics, particularly those processed from acetone/acetic acid, making them promising candidates for applications requiring surface wettability, such as filtration, biomedical scaffolds, or hydrophilic coatings.

6.4 Swelling

To further investigate the hydrophilic nature and water absorption behavior of the electrospun CA membranes, swelling capacity tests were conducted using fiber mats produced from three optimized formulations: 10 wt% CA in acetone, 15 wt% CA in acetone/acetic acid (2:1), and 18 wt% CA in acetone/DMF (2:1). These formulations were selected based on their ability to consistently produce uniform, bead-free fibers with desirable morphological characteristics. For the swelling analysis, 2×2 cm² sections of the electrospun mats were immersed in 30 mL of distilled water at room temperature for 24 h. The swelling capacity was quantified by calculating the percentage increase in mass between the dry and fully hydrated fiber mats.

As presented in Table 4, all samples exhibited significant water uptake, reflecting the inherent hydrophilic nature of CA. Among the samples, the CA fibers produced from the acetone/acetic acid system demonstrated the highest swelling ratio. This behavior can be attributed to their finer fiber diameter and higher porosity, which allow for more efficient water absorption and retention. In contrast, the sample from the acetone/DMF system, despite having thicker

fibers, showed slightly lower swelling capacity, likely due to reduced surface area and lower pore volume.

These findings align with previous studies reporting that fiber morphology, particularly diameter and porosity, plays a critical role in water absorption behavior of electrospun mats. Smaller fiber diameters and a more interconnected porous network enhance capillary action and water retention, thereby increasing swelling capacity. Moreover, the polar nature of acetic acid as a co-solvent may enhance the hydrophilicity of the resulting fibers, further promoting water uptake [57].

Overall, the swelling capacity results confirm that the solvent system and polymer concentration not only influence fiber formation but also directly impact the functional performance of CA membranes in aqueous environments. This property is particularly relevant for applications such as wound dressings, filtration media, and drug delivery systems, where high water absorption is desirable [24].

7 Conclusion

Solvent selection and concentration significantly influenced CA fiber size, distribution, and morphology. This study thoroughly investigated the effects of solvent mixture ratios and CA concentration on fiber and bead formation. Electrospinning CA solutions at low concentrations (5 wt%) in acetone, acetone/acetic acid (2:1), and acetone/DMF (2:1) resulted in clogging and bead formation. However, increasing polymer concentrations enabled the production of continuous, cylindrical fibers instead of beaded structures.

The addition of acetic acid to acetone improved CA electrospinnability, while a power-law relationship between fiber diameter and concentration was observed for the acetone/DMF system. Fiber diameters varied across solvent systems: 0.88–3.17 μm (acetone), 0.29–3.83 μm (acetone/acetic acid), and 0.32–0.79 μm (acetone/DMF), confirming that polymer concentration directly affects fiber diameter.

Optimal conditions for smooth, continuous fibers were achieved at 10 wt% (acetone), 15 wt% (acetone/acetic acid), and 18 wt% (acetone/DMF). Fiber morphology and wettability were highly dependent on diameter and solvent selection. As-spun CA fibers exhibited significant swelling (301–676%) after 24 h in water. Additionally, contact angles generally decreased with increasing polymer concentration. While fiber diameter does not always directly correlate with wettability, it influences surface properties such as roughness, pore size, and fiber orientation, which collectively determine wetting behavior.

Table 4 Swelling behavior of electrospun fibrous membranes of selected fiber after submersion in distilled water for 24 h

Solution system	Fiber diameter (μm)	Swelling (%)
18% acetone/DMF (2:1)	0.25	301
10% acetone	0.88	459
15% acetone/acetic acid (2:1)	2.21	676

Acknowledgement

The project presented in this article is supported by the National Research, Development, and Innovation Office—OTKA NKFI 146076. The authors sincerely thank

colleagues from HUN-REN Centre for Energy Research, Boglárka Ódor, Viktor Varga and Balázs Erki for helping us in carrying out the sample preparation, Dr. Tamás Kolonits for technical help in the SEM-EDS analysis of the samples.

References

- [1] Bhardwaj, N., Kundu, S. C. "Electrospinning: A fascinating fiber fabrication technique", *Biotechnology Advances*, 28(3), pp. 325–347, 2010.
<https://doi.org/10.1016/j.biotechadv.2010.01.004>
- [2] Kalaskar, D. M., Alshomer, F. "Chapter 8 - Micro- and Nanotopographical Cues Guiding Biomaterial Host Response", In: Lee, S. J., Yoo, J. J., Atala, A. (eds.) *In Situ Tissue Regeneration: Host Cell Recruitment and Biomaterial Design*, Academic Press, 2016, pp. 137–163. ISBN 978-0-12-802225-2
<https://doi.org/10.1016/B978-0-12-802225-2.00008-8>
- [3] Ahmadi Bonakdar, M., Rodrigue, D. "Electrospinning: Processes, Structures, and Materials", *Macromol*, 4(1), pp. 58–103.
<https://doi.org/10.3390/macromol4010004>
- [4] Sofi, H. S., Akram, T., Shabir, N., Vasita, R., Jadhav, A. H., Sheikh, F. A. "Regenerated cellulose nanofibers from cellulose acetate: Incorporating hydroxyapatite (HAP) and silver (Ag) nanoparticles (NPs), as a scaffold for tissue engineering applications", *Materials Science and Engineering: C*, 118, 111547, 2021.
<https://doi.org/10.1016/j.msec.2020.111547>
- [5] Alkaron, W., Almansoori, A., Balázs, K., Balázs, C. "Hydroxyapatite-Based Natural Biopolymer Composite for Tissue Regeneration", *Materials*, 17(16), 4117, 2024.
<https://doi.org/10.3390/ma17164117>
- [6] Gouma, P., Xue, R., Goldbeck, C. P., Perrotta, P., Balázs, C. "Nano-hydroxyapatite—Cellulose acetate composites for growing of bone cells", *Materials Science and Engineering: C*, 32(3), pp. 607–612, 2012.
<https://doi.org/10.1016/j.msec.2011.12.019>
- [7] Thomas, R. T., Del Río de Vicente, J. I., Zhang, K., Karzarjeddi, M., Liimatainen, H., Oksman, K. "Size exclusion and affinity-based removal of nanoparticles with electrospun cellulose acetate membranes infused with functionalized cellulose nanocrystals", *Materials & Design*, 217, 110654, 2022.
<https://doi.org/10.1016/j.matdes.2022.110654>
- [8] Li, A., Han, Z., Li, Z., Li, J., Li, X., Zhang, Z. "A PTHrP-2 loaded adhesive cellulose acetate nanofiber mat as wound dressing accelerates wound healing", *Materials & Design*, 212, 110241, 2021.
<https://doi.org/10.1016/j.matdes.2021.110241>
- [9] Pereira, A. G. B., Fajardo, A. R., Gerola, A. P., Rodrigues, J. H. S., Nakamura, C. V., Muniz, E. C., Hsieh, Y.-L. "First report of electrospun cellulose acetate nanofibers mats with chitin and chitosan nanowhiskers: Fabrication, characterization, and antibacterial activity", *Carbohydrate Polymers*, 250, 116954, 2020.
<https://doi.org/10.1016/j.carbpol.2020.116954>
- [10] Alkaron, W., Almansoori, A., Balázs, C., Balázs, K. "A Critical Review of Natural and Synthetic Polymer-Based Biological Apatite Composites for Bone Tissue Engineering", *Journal of Composites Science*, 8(12), 523, 2024.
<https://doi.org/10.3390/jcs8120523>
- [11] Zimmermann, L., Dombrowski, A., Völker, C., Wagner, M. "Are bioplastics and plant-based materials safer than conventional plastics? *In vitro* toxicity and chemical composition", *Environment International*, 145, 106066, 2020.
<https://doi.org/10.1016/j.envint.2020.106066>
- [12] Cramariuc, B., Cramariuc, R., Scarlet, R., Manea, L. R., Lupu, I. G., Cramariuc, O. "Fiber diameter in electrospinning process", *Journal of Electrostatics*, 71(3), pp. 189–198, 2013.
<https://doi.org/10.1016/j.elstat.2012.12.018>
- [13] Naragund, V. S., Panda, P. K. "Electrospinning of cellulose acetate nanofiber membrane using methyl ethyl ketone and N, N-Dimethylacetamide as solvents", *Materials Chemistry and Physics*, 240, 122147, 2020.
<https://doi.org/10.1016/j.matchemphys.2019.122147>
- [14] Korycka, P., Mirek, A., Kramek-Romanowska, K., Grzeczko, M., Lewińska, D. "Effect of electrospinning process variables on the size of polymer fibers and bead-on-string structures established with a 2³ factorial design", *Beilstein Journal of Nanotechnology*, 9, pp. 2466–2478, 2018.
<https://doi.org/10.3762/bjnano.9.231>
- [15] Al-Abduljabbar, A., Farooq, I. "Electrospun Polymer Nanofibers: Processing, Properties, and Applications", *Polymers*, 15(1), 65, 2023.
<https://doi.org/10.3390/polym15010065>
- [16] Han, S. O., Youk, J. H., Min, K. D., Kang, Y. O., Park, W. H. "Electrospinning of cellulose acetate nanofibers using a mixed solvent of acetic acid/water: Effects of solvent composition on the fiber diameter", *Materials Letters*, 62(4–5), pp. 759–762, 2008.
<https://doi.org/10.1016/j.matlet.2007.06.059>
- [17] Ghorani, B., Russell, S. J., Goswami, P. "Controlled Morphology and Mechanical Characterisation of Electrospun Cellulose Acetate Fibre Webs", *International Journal of Polymer Science*, 2013(1), 256161, 2013.
<https://doi.org/10.1155/2013/256161>
- [18] Maher Mehanna, M. "Electrospun Fibrous Mat of Cellulose Acetate: Influence of Solvent System (Acetic Acid/Acetone) on Fibers Morphology", *International Journal of Pharmaceutical Investigation*, 10(1), pp. 82–85, 2020.
<https://doi.org/10.5530/ijpi.2020.1.15>
- [19] Liu, H., Tang, C. "Electrospinning of Cellulose Acetate in Solvent Mixture *N,N*-Dimethylacetamide (DMAc)/Acetone", *Polymer Journal*, 39(1), pp. 65–72, 2007.
<https://doi.org/10.1295/polymj.PJ2006117>
- [20] Mikaeili, F., Gouma, P. I. "Super Water-Repellent Cellulose Acetate Mats", *Scientific Reports*, 8(1), 12472, 2018.
<https://doi.org/10.1038/s41598-018-30693-2>

- [21] Selatile, M. K., Ray, S. S., Ojijo, V., Sadiku, R. "Recent developments in polymeric electrospun nanofibrous membranes for sea-water desalination", *RSC Advances*, 8(66), pp. 37915–37938, 2018. <https://doi.org/10.1039/C8RA07489E>
- [22] Rasband, W. S., National Institutes of Health "Image Processing and Analysis in Java Program, (ImageJ 1.x)", [computer program] Available at: <http://imagej.nih.gov/ij> [Accessed: 20 March 2025]
- [23] Zhang, W., Vinueza, N. R., Datta, P., Michielsen, S. "Functional dye as a comonomer in a water-soluble polymer", *Journal of Polymer Science Part A: Polymer Chemistry*, 53(13), pp. 1594–1599, 2015. <https://doi.org/10.1002/pola.27592>
- [24] Tungprapa, S., Puangparn, T., Weerasombut, M., Jangchud, I., Fakum, P., Semongkhon, S., Meechaisue, C., Supaphol, P. "Electrospun cellulose acetate fibers: effect of solvent system on morphology and fiber diameter", *Cellulose*, 14(6), pp. 563–575, 2007. <https://doi.org/10.1007/s10570-007-9113-4>
- [25] Jaeger, R., Bergshoeff, M. M., Batlle, C. M. I., Schönherr, H., Julius Vancso, G. "Electrospinning of ultra-thin polymer fibers", *Macromolecular Symposia*, 127(1), pp. 141–150, 1998. <https://doi.org/10.1002/masy.19981270119>
- [26] Liu, H., Hsieh, Y.-L. "Ultrafine fibrous cellulose membranes from electrospinning of cellulose acetate", *Journal of Polymer Science Part B: Polymer Physics*, 40(18), pp. 2119–2129, 2002. <https://doi.org/10.1002/polb.10261>
- [27] Shenoy, S. L., Bates, W. D., Frisch, H. L., Wnek, G. E. "Role of chain entanglements on fiber formation during electrospinning of polymer solutions: good solvent, non-specific polymer–polymer interaction limit", *Polymer*, 46(10), pp. 3372–3384, 2005. <https://doi.org/10.1016/j.polymer.2005.03.011>
- [28] Hohman, M. M., Shin, M., Rutledge, G., Brenner, M. P. "Electrospinning and electrically forced jets. I. Stability theory", *Physics of Fluids*, 13(8), pp. 2201–2220, 2001. <https://doi.org/10.1063/1.1383791>
- [29] Merchiers, J., Meurs, W., Deferme, W., Peeters, R., Buntinx, M., Reddy, N. K. "Influence of Polymer Concentration and Nozzle Material on Centrifugal Fiber Spinning", *Polymers*, 12(3), 575, 2020. <https://doi.org/10.3390/polym12030575>
- [30] Kanjanapongkul, K., Wongsasulak, S., Yoovidhya, T. "Prediction of clogging time during electrospinning of zein solution: Scaling analysis and experimental verification", *Chemical Engineering Science*, 65(18), pp. 5217–5225, 2010. <https://doi.org/10.1016/j.ces.2010.06.018>
- [31] Sayed, N. M., Noby, H., Thu, K., El-Shazly, A. H. "High molecular weight cellulose acetate membrane electrospinning: Parameters experimental optimization", *Mater Today: Proceedings*, in press. (Accepted for publication: 29 August 2023) <https://doi.org/10.1016/j.matpr.2023.08.323>
- [32] Kramar, A., González-Benito, J. "Preparation of cellulose acetate film with dual hydrophobic-hydrophilic properties using solution blow spinning", *Materials & Design*, 227, 111788, 2023. <https://doi.org/10.1016/j.matdes.2023.111788>
- [33] Khoshnevisan, K., Maleki, H., Samadian, H., Shahsavari, S., Sarrafzadeh, M. H., Larijani, B., Dorkoosh, F. A., Haghpanah, V., Khorramzadeh, M. R. "Cellulose acetate electrospun nanofibers for drug delivery systems: Applications and recent advances", *Carbohydrate Polymers*, 198, pp. 131–141, 2018. <https://doi.org/10.1016/j.carbpol.2018.06.072>
- [34] Taepaiboon, P., Rungsardthong, U., Supaphol, P. "Vitamin-loaded electrospun cellulose acetate nanofiber mats as transdermal and dermal therapeutic agents of vitamin A acid and vitamin E", *European Journal of Pharmaceutics and Biopharmaceutics*, 67(2), pp. 387–397, 2007. <https://doi.org/10.1016/j.ejpb.2007.03.018>
- [35] Deitzel, J. M., Kleinmeyer, J., Harris, D., Beck Tan, N. C. "The effect of processing variables on the morphology of electrospun nanofibers and textiles", *Polymer*, 42(1), pp. 261–272, 2001. [https://doi.org/10.1016/S0032-3861\(00\)00250-0](https://doi.org/10.1016/S0032-3861(00)00250-0)
- [36] Angel, N., Guo, L., Yan, F., Wang, H., Kong, L. "Effect of processing parameters on the electrospinning of cellulose acetate studied by response surface methodology", *Journal of Agriculture and Food Research*, 2, 100015, 2020. <https://doi.org/10.1016/j.jafr.2019.100015>
- [37] Fong, H., Chun, I., Reneker, D. H. "Beaded nanofibers formed during electrospinning", *Polymer*, 40(16), pp. 4585–4592, 1999. [https://doi.org/10.1016/S0032-3861\(99\)00068-3](https://doi.org/10.1016/S0032-3861(99)00068-3)
- [38] Kong, L., Ziegler, G. R. "Rheological aspects in fabricating pul-lulan fibers by electro-wet-spinning", *Food Hydrocolloids*, 38, pp. 220–226, 2014. <https://doi.org/10.1016/j.foodhyd.2013.12.016>
- [39] Martins, A., Cunha, J., Macedo, F., Reis, R. L., Neves, N. M. "Improvement of Polycaprolactone Nanofibers Topographies: Testing the Influence in Osteoblastic Proliferation", In: 2006 NSTI Nanotechnology Conference and Trade Show (NSTI-Nanotech 2006), Boston, MA, USA, 2004, pp. 148–151. ISBN 0-9767985-7-3
- [40] Ryu, Y. J., Kim, H. Y., Lee, K. H., Park, H. C., Lee, D. R. "Transport properties of electrospun nylon 6 nonwoven mats", *European Polymer Journal*, 39(9), pp. 1883–1889, 2003. [https://doi.org/10.1016/S0014-3057\(03\)00096-X](https://doi.org/10.1016/S0014-3057(03)00096-X)
- [41] Amariei, N., Manea, L. R., Berteau, A. P., Berteau, A., Popa, A. "The Influence of Polymer Solution on the Properties of Electrospun 3D Nanostructures", *IOP Conference Series: Materials Science and Engineering*, 209(1), 012092, 2017. <https://doi.org/10.1088/1757-899X/209/1/012092>
- [42] Theron, S. A., Yarin, A. L., Zussman, E., Kroll, E. "Multiple jets in electrospinning: experiment and modeling", *Polymer*, 46(9), pp. 2889–2899, 2005. <https://doi.org/10.1016/j.polymer.2005.01.054>
- [43] Abdhussain, R., Adebisi, A., Conway, B. R., Asare-Addo, K. "Electrospun nanofibers: Exploring process parameters, polymer selection, and recent applications in pharmaceuticals and drug delivery", *Journal of Drug Delivery Science and Technology*, 90, 105156, 2023. <https://doi.org/10.1016/j.jddst.2023.105156>
- [44] Mit-uppatham, C., Nithitanakul, M., Supaphol, P. "Ultrafine Electrospun Polyamide-6 Fibers: Effect of Solution Conditions on Morphology and Average Fiber Diameter", *Macromolecular Chemistry and Physics*, 205(17), pp. 2327–2338, 2004. <https://doi.org/10.1002/macp.200400225>
- [45] Reneker, D. H., Yarin, A. L. "Electrospinning jets and polymer nanofibers", *Polymer*, 49(10), pp. 2387–2425, 2008. <https://doi.org/10.1016/j.polymer.2008.02.002>

- [46] Huang, Z.-M., Zhang, Y.-Z., Kotaki, M., Ramakrishna, S. "A review on polymer nanofibers by electrospinning and their applications in nanocomposites", *Composites Science and Technology*, 63(15), pp. 2223–2253, 2003.
[https://doi.org/10.1016/S0266-3538\(03\)00178-7](https://doi.org/10.1016/S0266-3538(03)00178-7)
- [47] Son, W. K., Youk, J. H., Lee, T. S., Park, W. H. "Electrospinning of ultrafine cellulose acetate fibers: Studies of a new solvent system and deacetylation of ultrafine cellulose acetate fibers", *Journal of Polymer Science Part B: Polymer Physics*, 42(1), pp. 5–11, 2004.
<https://doi.org/10.1002/polb.10668>
- [48] McKee, M. G., Wilkes, G. L., Colby, R. H., Long, T. E. "Correlations of Solution Rheology with Electrospun Fiber Formation of Linear and Branched Polyesters", *Macromolecules*, 37(5), pp. 1760–1767, 2004.
<https://doi.org/10.1021/ma035689h>
- [49] Koski, A., Yim, K., Shivkumar, S. "Effect of molecular weight on fibrous PVA produced by electrospinning", *Materials Letters*, 58(3–4), pp. 493–497, 2004.
[https://doi.org/10.1016/S0167-577X\(03\)00532-9](https://doi.org/10.1016/S0167-577X(03)00532-9)
- [50] Chau, T. T. "A review of techniques for measurement of contact angles and their applicability on mineral surfaces", *Minerals Engineering*, 22(3), pp. 213–219, 2009.
<https://doi.org/10.1016/j.mineng.2008.07.009>
- [51] Coverdale, B. D. M., Gough, J. E., Sampson, W. W., Hoyland, J. A. "Use of lecithin to control fiber morphology in electrospun poly (ϵ -caprolactone) scaffolds for improved tissue engineering applications", *Journal of Biomedical Materials Research Part A*, 105(10), pp. 2865–2874, 2017.
<https://doi.org/10.1002/jbma.a.36139>
- [52] Koombhongse, S., Liu, W., Reneker, D. H. "Flat polymer ribbons and other shapes by electrospinning", *Journal of Polymer Science Part B: Polymer Physics*, 39(21), pp. 2598–2606, 2001.
<https://doi.org/10.1002/polb.10015>
- [53] Norgren, M., Costa, C., Alves, L., Dahlström, C., Svanedal, I., Edlund, H., Medronho, B. "Perspectives on the Lindman Hypothesis and Cellulose Interactions", *Molecules*, 28(10), 4216, 2023.
<https://doi.org/10.3390/molecules28104216>
- [54] Honti, B., Fábrián, B., Idrissi, A., Jedlovsky, P. "Surface Properties of *N,N*-Dimethylformamide–Water Mixtures, As Seen from Computer Simulations", *The Journal of Physical Chemistry B*, 127(4), pp. 1050–1062, 2023.
<https://doi.org/10.1021/acs.jpcc.2c07572>
- [55] Thielke, M. W., Lopez Guzman, S., Victoria Tafoya, J. P., García Tamayo, E., Castro Herazo, C. I., Hosseinaei, O., Sobrido, A. J. "Full Lignin-Derived Electrospun Carbon Materials as Electrodes for Supercapacitors", *Frontiers in Materials*, 9, 859872, 2022.
<https://doi.org/10.3389/fmats.2022.859872>
- [56] Rbihi, S., Aboulouard, A., Laallam, L., Jouaiti, A. "Contact Angle Measurements of Cellulose based Thin Film composites: wettability, surface free energy and surface hardness", *Surfaces and Interfaces*, 21, 100708, 2020.
<https://doi.org/10.1016/j.surfin.2020.100708>
- [57] Milleret, V., Hefti, T., Hall, H., Vogel, V., Eberli, D. "Influence of the fiber diameter and surface roughness of electrospun vascular grafts on blood activation", *Acta Biomaterialia*, 8(12), pp. 4349–4356, 2012.
<https://doi.org/10.1016/j.actbio.2012.07.032>
- [58] Samaha, M. A., Gad-el-Hak, M. "Polymeric Slippery Coatings: Nature and Applications", *Polymers*, 6(5), pp. 1266–1311, 2014.
<https://doi.org/10.3390/polym6051266>
- [59] Kontturi, E., Johansson, L.-S., Kontturi, K. S., Ahonen, P., Thüne, P. C., Laine, J. "Cellulose Nanocrystal Submonolayers by Spin Coating", *Langmuir*, 23(19), pp. 9674–9680, 2007.
<https://doi.org/10.1021/la701262x>